



Short communication

A nanostructure anode ($\text{Cu}_{0.2}\text{Zn}_{0.8}$) for low-temperature solid oxide fuel cell at 400–600 °CRizwan Raza^{a,b,*}, Xiaodi Wang^c, Ying Ma^c, Bin Zhu^{a,d}^a Department of Energy Technology, Royal Institute of Technology (KTH), 10044 Stockholm, Sweden^b Department of Physics, COMSATS University, Lahore 54000, Pakistan^c Division of Functional Materials, Royal Institute of Technology (KTH), 16440 Stockholm, Sweden^d GETT Fuel Cells International AB, Stora Nygatan 33, S-10314 Stockholm, Sweden

ARTICLE INFO

Article history:

Received 1 March 2010

Accepted 18 July 2010

Available online 22 July 2010

Keywords:

Low temperature

Ceramic fuel cell

Nanoparticles

Catalyst

ABSTRACT

We developed a new nickel-free anode for a low-temperature solid oxide fuel cell (LTSOFC) that demonstrated an outstanding electrochemical output of 1000 mW cm^{-2} at 550 °C. The nanostructure anode had good conductivity and was compatible with cerium oxide-based electrolytes. The performance of a single cell was comparable and or better than those using standard Ni-YSZ and Ni-SDC electrodes (anode). It may have applications for hydrocarbon-based fuel for preventing carbon deposition and replacing nickel in the anode of LTSOFCs.

© 2010 Elsevier B.V. All rights reserved.

1. Introduction

Nanostructure materials are undergoing intense research in the areas of solid-state chemistry, physics, and ionics; materials engineering; medical science; and biotechnology [1]. Newly developed energy conversion devices must meet today's demand for energy efficiency, affordability, and environmental safety. An effective way to develop new materials for these devices is to use nanostructure materials [2,3]. Nanosized particles may enhance the cell's catalytic properties and the reactive area, which would increase the ionic and electronic conductivity [4]. The current intense research activity on solid oxide fuel cells (SOFCs) is important because of their considerable energy efficiency and environmental benefits. To commercialise SOFCs, researchers have sought to reduce the operating temperature of these by developing a new electrolyte with high ionic conductivity and electrodes with high electronic conductivity [5,6]. However, the operation of SOFCs remains costly using these methods, and a reduction in operating temperature would significantly reduce their component costs (including interconnects, sealing materials, and manifold materials) and their manufacturing costs [3–8].

In the race to develop new nanocomposite materials for low-temperature (300–600 °C) applications, researchers have introduced new electrolytes and electrodes [1–10] but have not yet developed a compatible electrode that works efficiently at low temperatures.

Another very important issue concerns anodes. Nickel-containing composite electrodes, including Ni-YSZ and Ni-SDC and others, have shortcomings, including carbon deposition and degradation [7,11]. These shortcomings can be avoided by the developing carbon-resistant electrocatalysts that have high catalytic activity [7].

Although LTSOFC electrolytes have high ionic and electronic anode conductivity, there are important issues concerning the electrode's morphology and electrolyte's compatibility at low temperatures [7–10]. As Selman [10] expressed, "alternatives to nickel-based electro catalysts are being pursued to circumvent the problems contributing to the performance degradation of high-temperature fuel cells."

Each component in the SOFC is very important for enhancing the performance of the fuel cell in terms of morphology, conductivity and, compatibly with each other. These factors can also reduce the operating temperature of the fuel cell [9]. To achieve high performance, the anode must have a fine particle size, large surface area, adequate porosity, and sufficient Ni content [4,12].

The purpose of this paper is to develop nickel-free nanostructure conducting metal oxide anodes for SOFCs [12] that work well at very low temperatures and possibly demonstrate carbon resistance. Therefore, we developed such electrodes for low-temperature

* Corresponding author at: Department of Energy Technology, Royal Institute of Technology (KTH), Brinellvägen 68, Heat and Power Division, 10044 Stockholm, Sweden. Tel.: +46 762569336; fax: +46 8204161.

E-mail address: razahussaini786@gmail.com (R. Raza).

(300–600 °C) solid oxide fuel cells (LT-SOFCs) and characterised them by scanning electron microscopy (SEM), transmission electron microscopy (TEM), and X-ray diffraction (XRD). We compared the anodes' performance with that of conventional anode material. We used the new product for an advanced nanocomposite electrolyte to construct fuel cells and analysed the performance of the anode material. The anode stability, electrochemical performance, and AC impedance were also examined at different temperatures.

2. Experimental procedure

2.1. Electrode preparation

The nanostructure anode was prepared by a solid-state reaction. A stoichiometric amount of CuCO_3 (99.99%, Aldrich) and ZnNO_3 (99.99%, Aldrich) were mixed and ground in a mortar. The CuCO_3 and ZnNO_3 were precalcined at 700 °C for 3 h to remove the carbonates and hydroxides and then were mixed with samarium doped ceria (SDC) nanocomposite electrolyte ($\text{SDC-Na}_2\text{CO}_3$ or NSDC) in one step in a 1:1 volumetric ratio [13,14]. This powder was sintered for 4 h at 800 °C in a furnace.

Two cells, 13 mm in diameter and 0.8 mm thick, were fabricated using the co-pressing process with two different anodes (one conventional and a second with our prepared materials). The first and second cells of the sintered powder were fabricated with symmetrical order anode ($\text{CuZn-NSDC/NSDC/cathode}$ (conventional)) and anode ($\text{Ni-NSDC/NSDC/cathode}$ (conventional)), respectively, by dry pressing at 250 MPa using a stainless-steel die. The cells were sintered at 650 °C in air for 30 min.

To measure the fuel cells' performance, anode and cathode surfaces were painted with silver to collect current data. The active area of the fuel cell was 0.64 cm² and tested at temperatures from 400 °C to 580 °C using hydrogen as a fuel and stationary air as the oxidant. The gas flow rate ranged from 90 ml min⁻¹ to 110 ml min⁻¹ at 1 atm pressure. The electrochemical performance of the fuel cell was measured by a computerised instrument (L-43, made in China).

2.2. Microstructure analysis

The microstructural and morphological characterisations were studied using a Zeiss Ultra 55 field-emission SEM (FE-SEM). Additional data on the morphology, nanostructure, and particle size were determined using TEM (JEOL JEM-2100F) on a carbon-coated copper grid.

2.3. Crystal structure analysis

The phase and crystal structure analysis was conducted using XRD (D/Max-3A Regaku x-ray diffractometer) with $\text{Cu K}\alpha$ radiation, 35 kV voltage, and a 30 mA current at room temperature at scanning rate of 0.005°. Surface area measurements (BET, Brunauer–Emmit–Teller) were made by nitrogen adsorption (Micromeritics ASAP 2000 instrument (Norcross, GA)). The mean particle size (D_{BET}) was calculated from the BET data according to the Scherrer equation, assuming that the particles were closed uniform spheres with a smooth surface.

2.4. Electrochemical analysis

Electrochemical impedance spectra (EIS) were measured at different temperatures in air from 0.1 MHz to 1 MHz, and the excitation voltage was fixed at 10 mV using an impedance analyser (VERASTA2273) and the potentiostatic technique. We used the ZSimpWin software for the curve fitting with an equivalent circuit and simulating the results of experimental data.

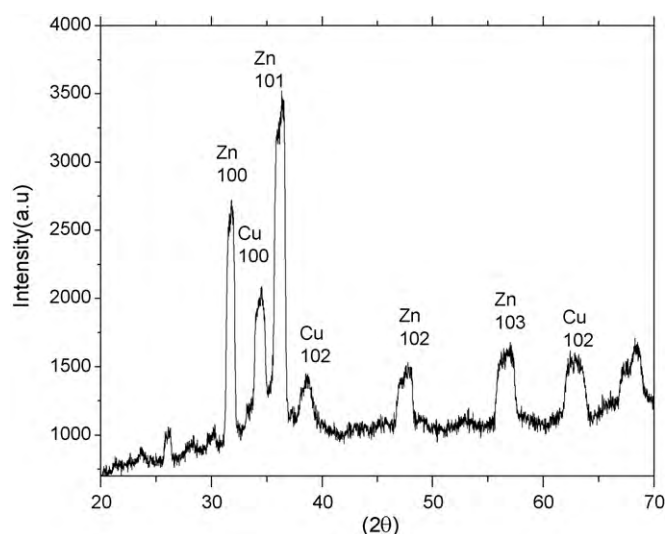


Fig. 1. XRD pattern for $\text{Cu}_{0.2}\text{Zn}_{0.8}\text{-NSDC}$.

3. Results and discussion

Our electrode preparation method produces large quantities inexpensively. In the CuZn-SDC anode, the small Cu particle size might be important to catalytic activity [15]. The function of ZnO is to alter the electronic states of these particles for improved catalytic activity.

The XRD pattern is presented in Fig. 1, which shows the significant reaction occurring between CuO and ZnO . The as-prepared oxides possessed a perovskite phase structure with CuO incorporated into a phase. The XRD peaks were observed for oxides. These showed that a solid-state reaction occurred between the oxides and included two highly crystalline phases. The crystallite size was 20 nm, determined using the Scherrer equation. Based on the BET results, the average electrode particle size was 20–50 nm. The S_{BET} was the measured specific surface area expressed as 2.71 m² g⁻¹.

Fig. 2(a) shows the SEM results where the nanostructure and morphology of the particle was more homogeneous. The interparticle connectivity was much better and produced a uniform and porous structure. The optimal sintering temperature (800 °C for 4 h) resulted in this type of morphology and performed well.

The optimised microstructure will be the best improvement in the anode properties.

The fine particle size distribution (about 50–100 nm), the adequate porosity, and the amount of well-connected Cu and Zn all contributed to the fuel cell's high performance.

These well-connected CuZn nanoparticles and relatively high-content Zn phase in the composite electrode and anode enhanced the electronic conduction, which helped the H_2 oxidation. The $\text{SDC-Na}_2\text{CO}_3$ electrolyte particles served as the main oxygen ion conduction supplier.

The purpose of mixing the 50% electrolyte volume in the composite anode was to increase the oxidation (ionic conductivity) from the anode to the interior of the solid electrolytes and to minimise the interfacial resistance crossover of the anode/electrolyte interface. The composite anode was porous, which allowed the gas to be thoroughly distributed in the anode to the electrolyte in the fuel cell. These properties enabled the high fuel cell performance at low temperatures.

The TEM results of the nanocomposite anode are shown in Fig. 2(b) and (c). The particle sizes ranged from 5 nm to 20 nm. The microstructure revealed a large reaction site. Fig. 3 shows that 10-nm hexagonal Zn was thoroughly mixed with the 5-nm Cu particles, which was confirmed by the crystal lattice calculations from the

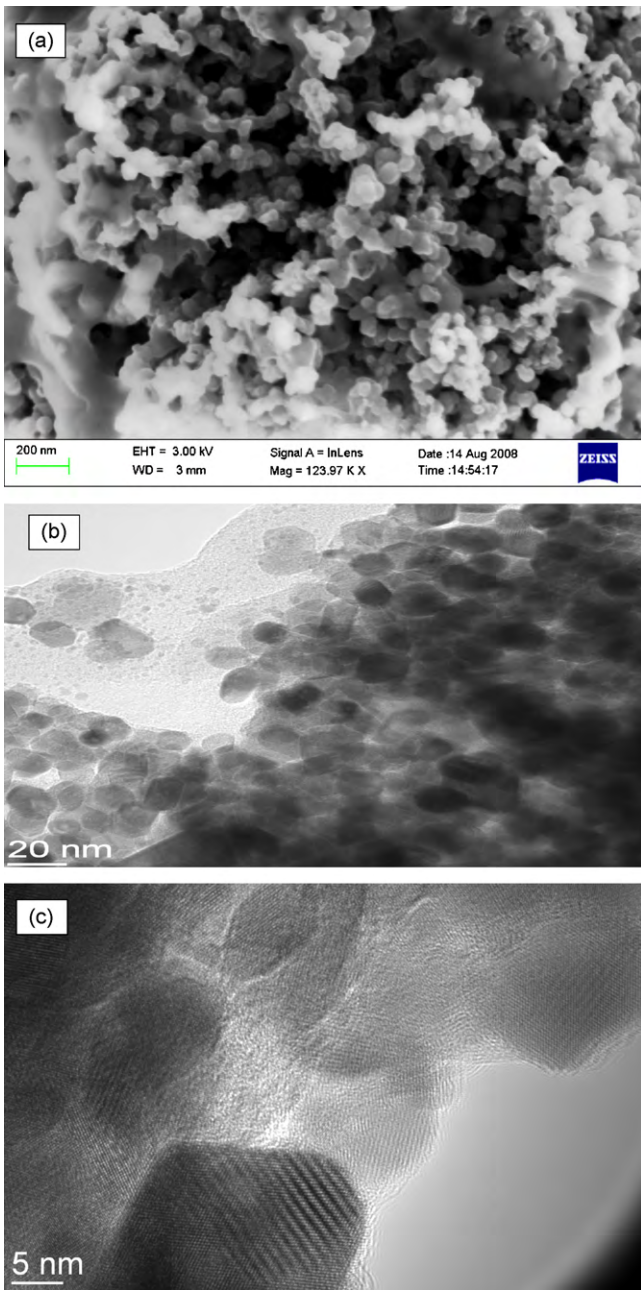


Fig. 2. (a) SEM images of $\text{Cu}_{0.2}\text{Zn}_{0.8}\text{-NSDC}$. (b and c) High-resolution TEM images.

high-resolution TEM images. This close-packed hexagonal inter-connected anode structure facilitated the diffusion of fuel/oxidant to the interface of the electrolyte and electrodes. These results showed excellent agreement with the SEM and XRD particle size calculations. The pores between the particles ranged from 5 nm to 50 nm.

Fuel cell performance of conventional anodes and our Ni-free anodes (Ni-NSDC and CuZn-NSDC) were compared and the results are shown in Fig. 3(a) and (b). Note that the fuel cells shown in Fig. 3(b) had a higher power density, whereas the open circuit voltage (OCV) is the same. The OCV and peak power densities shown in Fig. 3(b) were 1000 mW cm^{-2} at 550°C . The outstanding fuel cell performance was comparable to those using Ni-YSZ and Ni-SDC or other Ni-based anodes but at much lower temperatures, i.e., 400°C in this work. The advantages of this nanostructure are obvious, as were the good interconnections between the nanopar-

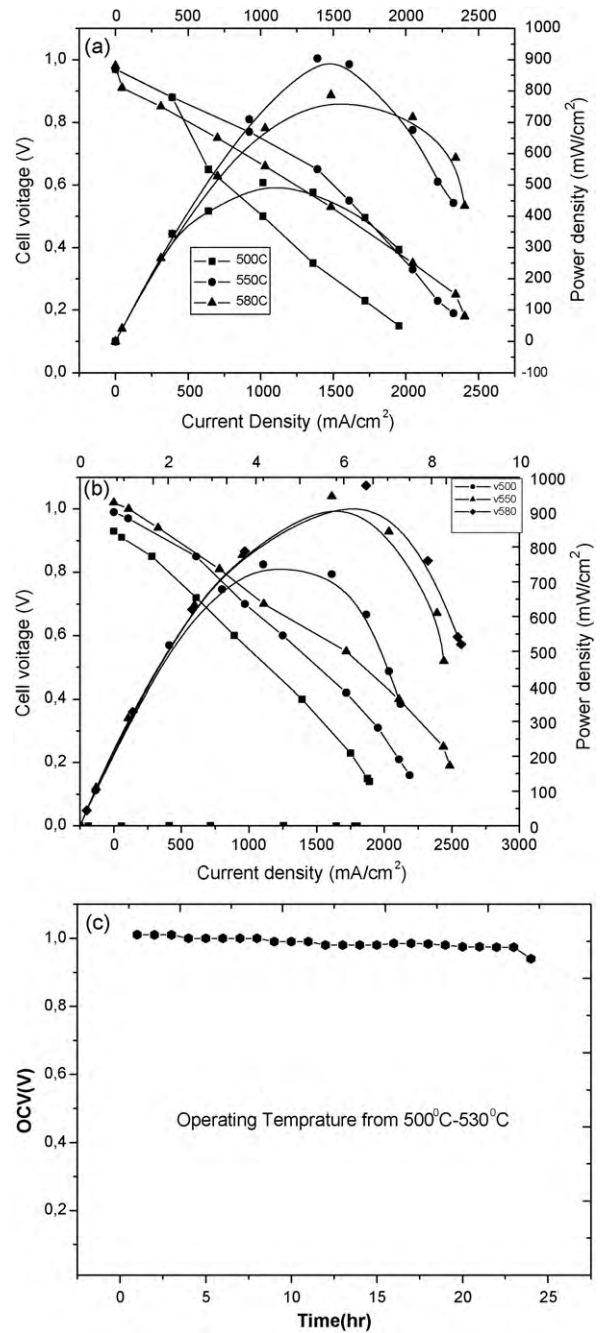


Fig. 3. $I-V/I-P$ characteristics of a fuel cell at different temperatures. (a) Anode (Ni-NSDC). (b) Anode (CuZn-NSDC). (c) Power generation properties of SOFC (time evolution of the terminal voltage (OCV)).

ticles and interfaces. These results show that the prepared anode is compatible and can replace the nickel-based anodes.

Fig. 3(c) shows that the OCV of the single cell was very stable, 1.011 V, from 500°C to 530°C , measured over a 24-h period. The performance of this fuel cell was very good with the Ni-free anode, which also showed stability of the as-prepared anode material.

The experimental data were modelled with ZView software and a draw LRQ equivalent circuit shown inside Fig. 4. An inductance L may have the effect of a stainless tube of the measurement device. The R_1 electrochemical resistance was most likely related to the anode reaction. The R_2 was caused by the electrolytic resistance. Q was the constant phase element, mainly caused by the interfaces between the anode and electrolyte. R_2 decreased with

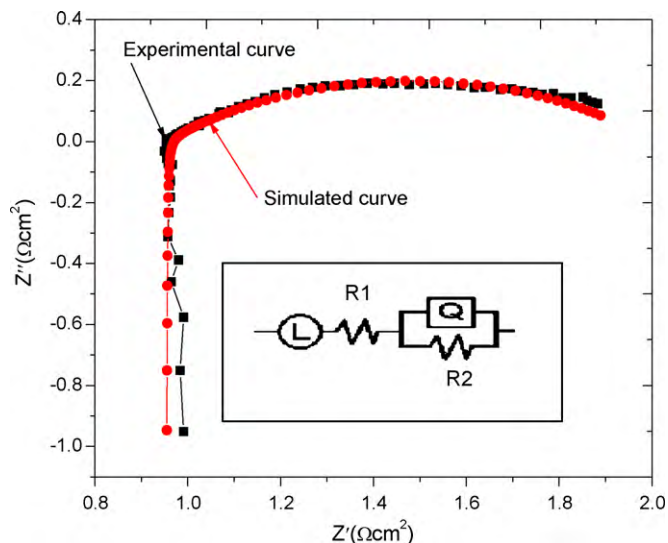


Fig. 4. AC impedance at 500 °C (FC1.0V open).

increasing of temperature, which was attributed to the increase of the material conductivity with temperature. The lower resistance (interfacial) of the electrolyte and electrode resulted in the high fuel cell performance. Thus, the development of compatible electrodes with high-catalyst activity significantly reduced the electrode polarisation losses and helped yield the high-performance low-temperature fuel cells.

4. Conclusion

The nanostructured anode reported in this work showed the excellent performance with an optimum mixture of two phases (electrolyte and electrode). The compatibility between both electrode and electrolyte materials was the basis for the development of an efficient high-catalyst, durable, and chemically stable electrode. It was also active and functioned at well at low tem-

peratures, 400–550 °C, with OCV stability between 1.011 V and 0.99 V.

We concluded that the nickel-free anode enabled a performance comparable to that seen with current nickel-based anodes and might be a good application for the LT-SOFC. It might be useful for avoiding carbon deposition during the internal reforming and fuel cell reactions. In addition, it could prevent catalyst deactivation in SOFC anodes when using the hydrocarbon fuels. We believe it will be further improved by optimising the nanostructure and composition of oxide elements.

Acknowledgements

This work is supported by the EC FP6 NANOCOFC project (contract no. 032308), Swedish Innovation System (VINNOVA), Swedish Research Council (VR)/Swedish agency for international cooperation development (Sida). The HEC, Pakistan also acknowledge for PhD scholarship.

References

- [1] J. Schoonman, *Solid State Ionics* 135 (2000) 5.
- [2] A. Salvatore Arico, P. Bruce, B. Scrosati, J.M. Tarascon, W. Schalkwijk, *Nat. Mater.* 41 (2005) 367.
- [3] B. Zhu, *Int. J. Energy Res.* 33 (2009) 1126.
- [4] T.Z. Sholklapper, H. Kurokawa, C.P. Jacobson, S.J. Visco, L.C. De Jonghe, *Nano Lett.* 7 (2007) 2136.
- [5] T. Suzuki, Z. Hasan, Y. Funahashi, T. Yamaguchi, Y. Fujishiro, M. Awano, *Science* 325 (2009) 852.
- [6] L. Bi, S. Zhang, S. Fang, Z. Tao, R. Peng, W. Liu, *Electrochem. Commun.* 10 (2008) 1598.
- [7] S.D. Kim, H. Moon, S.H. Hyun, J. Moon, J. Kim, H.W. Lee, *J. Power Sources* 163 (2006) 392.
- [8] I. Gavrielatos, V. Drakopoulos, S.G. Neophytides, *J. Catal.* 259 (2008) 75.
- [9] F. Zhao, A.V. Virkar, *J. Power Sources* 141 (2005) 79.
- [10] J.R. Selman, *Science* 326 (2009) 52.
- [11] S.D. Kim, H. Moon, S.H. Hyun, J. Moon, J. Kim, H.W. Lee, *J. Power Sources* 169 (2007) 265.
- [12] L. Yang, S. Wang, K. Blinn, M. Liu, Z. Liu, Z. Cheng, M. Liu, *Science* 326 (2009) 126.
- [13] R. Raza, X. Wang, Y. Ma, B. Zhu, *Int. J. Hydrogen Energy* 35 (2010) 2684.
- [14] X. Wang, Y. Ma, R. Raza, M. Muhammed, B. Zhu, *Electrochem. Commun.* 10 (2008) 1617.
- [15] K. Tohji, Y. Udagawa, T. Mizushima, A. Ueno, *J. Phys. Chem.* 89 (1985) 5671.